Available online at www.sciencedirect.com
SCIENCE DIRECT
Nuclear Medicine and Biology 32 (2005) 353–360
NUCLEAR MEDICINE — AND — BIOLOGY
www.elsevier.com/locate/nucmedbio

A preliminary PET evaluation of the new dopamine D_2 receptor agonist [^{11}C]MNPA in cynomolgus monkey

Sjoerd J. Finnema[a], Nicholas Seneca[a,c], Lars Farde[a], Evgeny Shchukin[c], Judit Sóvágó[a], Balázs Gulyás[a], Håkan V. Wikström[b], Robert B. Innis[c], John L. Neumeyer[d], Christer Halldin[a,*]

[a]*Department of Clinical Neuroscience, Psychiatry Section, Karolinska Institute, Karolinska University Hospital, S-17176 Stockholm, Sweden*
[b]*Department of Medicinal Chemistry, University Centre for Pharmacy, University of Groningen, Groningen, NL-9913 AV, The Netherlands*
[c]*Molecular Imaging Branch, National Institute of Mental Health, National Institutes of Health, Bethesda, MD 20892, USA*
[d]*Alcohol and Drug Abuse Research Center, McLean Division of Massachusetts General Hospital, Harvard Medical School, Belmont, MA 02478-9106, USA*

Received 28 October 2004; received in revised form 11 January 2005; accepted 19 January 2005

Abstract

This study describes the preliminary positron emission tomography (PET) evaluation of a dopamine D_2-like receptor agonist, (*R*)-2-$^{11}CH_3O$-*N*-*n*-propylnorapomorphine ([^{11}C]MNPA), as a potential new radioligand for in vivo imaging of the high-affinity state of the dopamine D_2 receptor (D_2R). MNPA is a selective D_2-like receptor agonist with a high affinity (K_i=0.17 nM). [^{11}C]MNPA was successfully synthesized by direct O-methylation of (*R*)-2-hydroxy-NPA using [^{11}C]methyl iodide and was evaluated in cynomolgus monkeys. This study included baseline PET experiments and a pretreatment study using unlabeled raclopride (1 mg/kg). High uptake of radioactivity was seen in regions known to contain high D_2R, with a maximum striatum-to-cerebellum ratio of 2.23±0.21 at 78 min and a maximum thalamus-to-cerebellum ratio of 1.37±0.06 at 72 min. The pretreatment study demonstrated high specific binding to D_2R by reducing the striatum-to-cerebellum ratio to 1.26 at 78 min. This preliminary study indicates that the dopamine agonist [^{11}C]MNPA has potential as an agonist radioligand for the D_2-like receptor and has potential for examination of the high-affinity state of the D_2R in human subjects and patients with neuropsychiatric disorders.
© 2005 Elsevier Inc. All rights reserved.

Keywords: Dopamine agonist; D_2 receptor; High-affinity state; PET; Monkey; [^{11}C]MNPA

1. Introduction

Studies of the dopaminergic system utilizing positron emission tomography (PET) have primarily focused on the use of antagonists, such as [^{11}C]raclopride [1]. High signal relies mainly on the fact that antagonists have equal binding affinity for receptors in both the high- and low-affinity states [2–6]. The use of antagonists to quantify receptor levels within the brain has been applied to examine the dopamine (DA) system in various psychiatric disorders. In addition to these studies, drug-induced receptor occupancy analysis has been used in drug development of antipsychotic drugs, themselves being antagonists, in order to demonstrate therapeutic efficacy.

A limitation with DA antagonists, however, is that they have no inherent potential to distinguish receptors in high- vs. low-affinity states as proportion varies with conditions. The study of neurotransmission is therefore very difficult because endogenous DA binds preferentially to receptors in the high-affinity state. An agonist radioligand may thus be more sensitive to endogenous DA levels when compared with an antagonist radioligand.

To overcome this limitation, studies aiming at the development of agonist radioligands have recently been undertaken [7–11]. Some of the most potent DA agonists identified thus far are apomorphine and its analogues [12,13]. One of the apomorphine analogues, (*R*)-*N*-^{11}C-propyl-norapomorphine ([^{11}C]NPA; Fig. 1), has been evaluated in baboon and showed a striatum-to-cerebellum ratio of 2.8 [8]. These developments of agonist radioligands are of particular interest since they may have increased sensitivity for endogenous DA levels. Immediate support for this hypoth-

* Corresponding author. Tel.: +46 8 51772678; fax: +46 8 51771753.
E-mail address: christer.halldin@cns.ki.se (C. Halldin).

0969-8051/$ – see front matter © 2005 Elsevier Inc. All rights reserved.
doi:10.1016/j.nucmedbio.2005.01.007

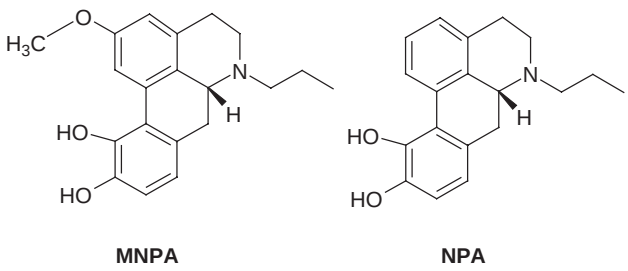

Fig. 1. Structures of MNPA (left) and NPA (right).

esis is found in an agonist–antagonist comparison, where an induced increase in synaptic DA due to acute amphetamine exposure resulted in a 42% higher decrease in [^{11}C]NPA binding, as compared to [^{11}C]raclopride binding [14].

Among the apomorphine analogues, (*R*)-2-CH_3O-*N*-*n*-propylnorapomorphine (MNPA; Fig. 1) has a very high D_2-like receptor binding affinity [1.02 nM (IC_{50}) or 0.17 nM (K_i)], as compared to NPA [4.80 nM (IC_{50}) or 0.8 nM (K_i)] [12,13]. A preliminary study in a cynomolgus monkey and with an old PET system has demonstrated a marked uptake in the striatum after iv injection of [^{11}C]MNPA. The striatum-to-cerebellum ratio was approximately 2, with accumulation of radioactivity in regions known to contain high dopamine D_2 receptor (D_2R) [15].

The aim of the present study was to optimize the radiosynthesis of [^{11}C]MNPA by direct methylation and to examine its potential as a radioligand. The specificity and selectivity of binding were examined by baseline and pretreatment experiments in cynomolgus monkeys. [^{11}C]MNPA metabolism was measured in monkey plasma by gradient HPLC.

2. Materials and methods

2.1. Radiochemistry

2.1.1. General procedures

Dimethyl sulfoxide (DMSO) and 5 M NaOH were obtained from Fluka Sweden and the Swedish Pharmacy, respectively. Additional chemicals were obtained from various commercial sources and were, whenever possible, of analytical grade. [^{11}C]Methane was produced with a GEMS PETtrace cyclotron at the Karolinska University Hospital, Stockholm, Sweden, using 16.4-MeV protons in the ^{14}N(p,α)^{11}C reaction on nitrogen gas containing 10% H_2. The target gas was irradiated for 20 min with a beam intensity of 35 μA. The synthesis and purification of [^{11}C]MNPA were performed in a fully automated methylation system in which [^{11}C]methyl iodide was prepared from [^{11}C]methane by gas-phase iodination [16]. Purification of [^{11}C]MNPA was performed using a semipreparative reversed-phase HPLC system, containing a Waters μ-Bondapak C-18 column (300×7.8 mm, 10 μm) and an absorbance detector (λ=254 nm) in series with a GM tube for radiation detection. [^{11}C]MNPA was purified by HPLC using acetonitrile and phosphoric acid (10 mM) (25:75 v:v) as mobile phase at a flow rate of 4 ml min^{-1}. The radiochemical purity of [^{11}C]MNPA was analyzed by reversed-phase HPLC using a Waters μ-Bondapak C-18 column (300×3.9 mm, 10 μm) and an absorbance detector (λ=254 nm) in series with a Beckman 170 β-flow radiodetector for radiation detection. Acetonitrile and phosphoric acid (10 mM) (25:75 v:v) were used as mobile phase with a flow rate of 2 ml/min. [^{11}C]MNPA was identified by coinjection with unlabeled MNPA.

2.1.2. Preparation of [^{11}C]MNPA

[^{11}C]Methyl iodide was trapped at room temperature in a reaction vessel containing 1.0 mg of (*R*)-2-hydroxy-NPA, DMSO (300 μl) and sodium hydroxide (5 M, 5 μl) (Fig. 2). The vessel was heated at 80°C for 5 min and the mobile phase (600 μl) was added to the crude reaction mixture. After injection into the semipreparative HPLC column, [^{11}C]MNPA eluted after 7–8 min (Fig. 3). After evaporation of the mobile phase, the residue was dissolved in 8 ml of sterile phosphate-buffered saline (pH 7.4) and filtered through a sterile Millipore filter (0.22 μm), yielding a sterile solution free from pyrogens. Further verification of the position of the O-alkylation has been performed by postderivatization of the catechol group of [^{11}C]MNPA resulting to the ^{11}C-labeled (*R*)-2-methoxy-10,11-diaceto-NPA or (*R*)-2-methoxy-10,11-methylendioxy-NPA (Fig. 4). (*R*)-2-Methoxy-10,11-diacetyl-NPA was formed by heating the crude [^{11}C]MNPA mixture with acetic anhydride and pyridine for 10 min at 100°C. (*R*)-2-Methoxy-10,11-methylendioxy-NPA was formed by adding dibromomethane (150 μl) to the crude [^{11}C]MNPA mixture and heating for 5 min at 95°C. The derivates were compared with the standard by coinjection on the analytical HPLC system.

2.2. PET measurements

Radioactivity in the brain was measured with the Siemens ECAT Exact HR47 system, which was used in the three-dimensional mode [17]. The system covers an axial distance of 15 cm. The transaxial resolution of the reconstructed images is about 3.8 mm full width at half-maximum (FWHM) and the axial resolution is 4.0 mm FWHM. The reconstructed volume was displayed as 47 transaxial sections, with a section thickness of 3.125 mm. Transmission scans were acquired with three rotating ^{68}Ge–^{68}Ga sources and were used to correct the emission scans for the attenuation of 511-keV photon rays through tissue and head support [17].

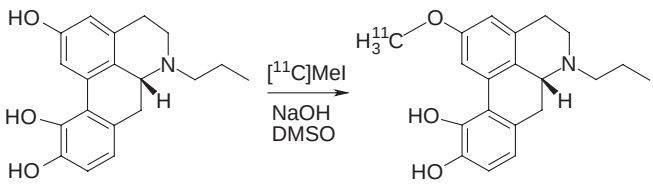

Fig. 2. Preparation of [^{11}C]MNPA.

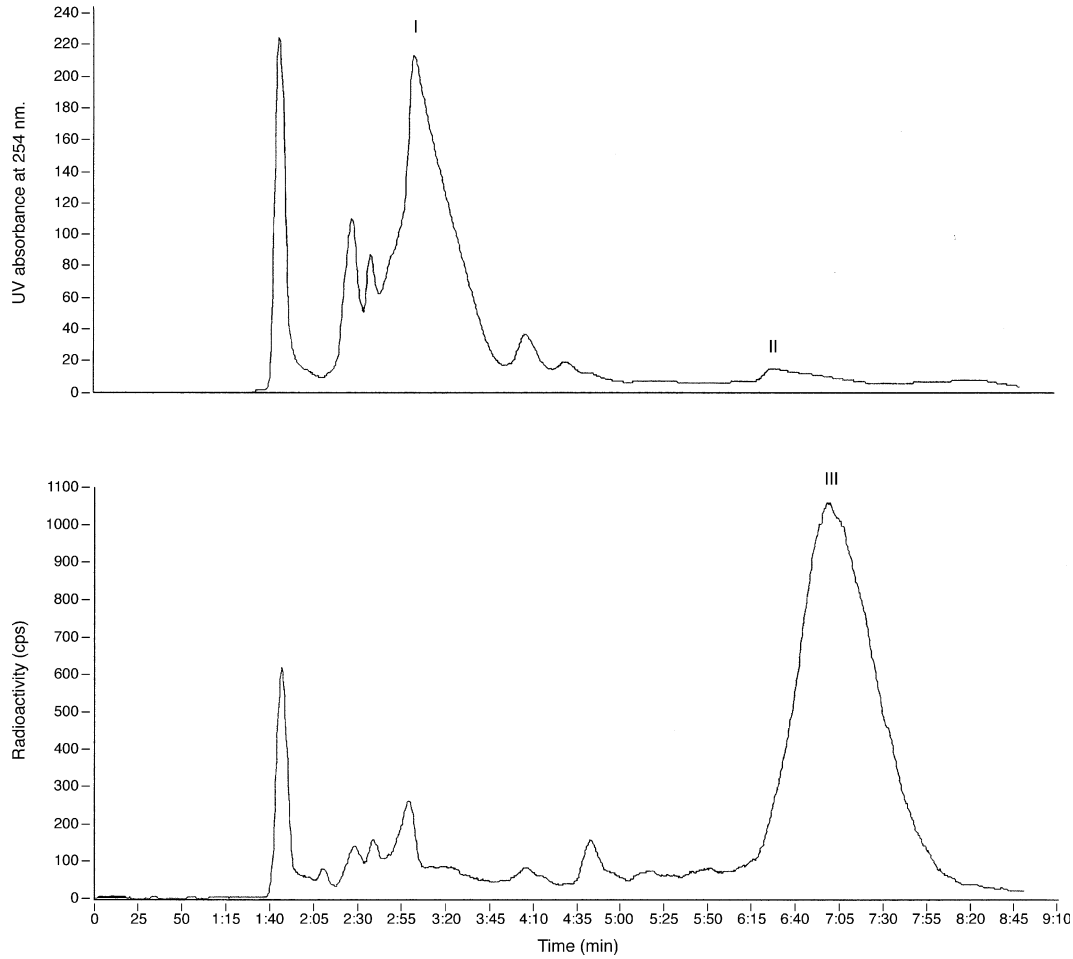

Fig. 3. Semipreparative HPLC chromatograms (UV and radioactivity vs. time) of the purification of [^{11}C]MNPA using a semipreparative reversed-phase HPLC column. (I) (*R*)-2-hydroxy-NPA, (II) MNPA and (III) [^{11}C]MNPA.

Two cynomolgus monkeys (6.5 and 7.6 kg) were supplied by the Astrid Fagræus Laboratory (Karolinska Institutet, Solna, Sweden). The study was approved by the Animal Research Ethical Committee of the Northern Stockholm Region. Anaesthesia was induced and maintained by repeated im injection of a mixture of ketamine (3–4 mg kg^{-1} h^{-1} Ketalar, Parke-Davis) and xylazine hydrochloride (1–2 mg kg^{-1} h^{-1} Rompun Vet., Bayer of Sweden) during the entire study session. A head fixation system was used to secure a fixed position of the monkey's head during the PET measurements [18]. The body temperature was controlled by Bair Hugger Model 505 (Arizant Healthcare, MN, USA).

Altogether, three PET measurements were performed in the two monkeys. In each PET measurement, 56–57 MBq of [^{11}C]MNPA was injected as a bolus into the left sural vein during 2 s, followed by an injection of saline (2 ml), with simultaneous start of PET-data acquisition. Radioactivity in the brain was measured according to a preprogrammed sequence of frames, up to 93 min after injection of [^{11}C]MNPA. In both monkeys, a baseline measurement was performed with [^{11}C]MNPA. In the second monkey, an additional measurement was performed in which 1 mg kg^{-1}

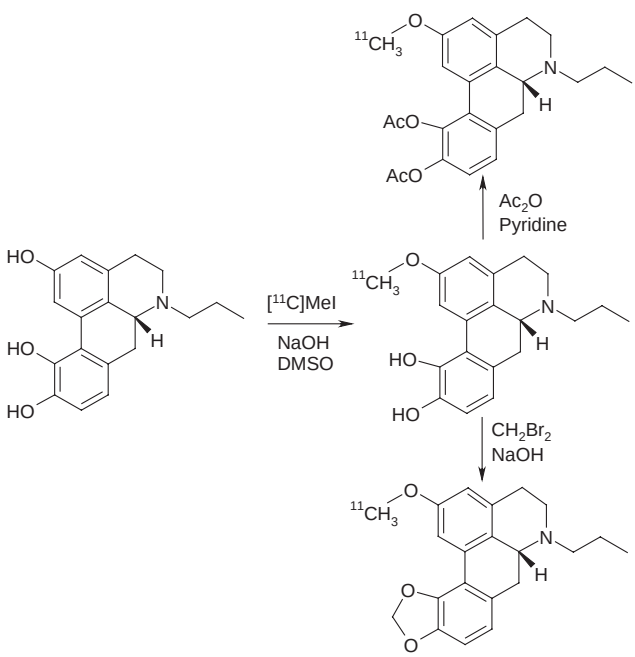

Fig. 4. Derivatization of [^{11}C]MNPA giving the ^{11}C-labeled (*R*)-2-methoxy-10,11-diaceto-NPA and (*R*)-2-methoxy-10,11-methylendioxy-NPA.

of the D_2R antagonist raclopride was injected iv 10 min prior to the injection of [^{11}C]MNPA.

2.2.1. Regions of interest

The regions of interest (ROIs) were drawn on PET summation images representing radioactivity measured from 9 min after iv injection of [^{11}C]MNPA to the end of the measurement. The caudate, putamen, thalamus, cerebellum and whole brain were defined according to an atlas of a cryosected cynomolgus monkey head in situ [18]. The images were then analyzed with PMOD 2.5, a pixel-wise modeling computer software (PMOD Group, Zurich, Switzerland.). For each region, radioactivity was calculated for the sequence of time frames, corrected for the radioactivity decay and plotted vs. time.

2.2.2. Quantitative analyses

To calculate the percentage of injected [^{11}C]MNPA present in the brain at the time of maximal radioactivity, the radioactivity concentration in the ROI for the whole brain was multiplied with an estimated brain volume of 65 ml for an adult cynomolgus monkey. The calculated value for total radioactivity in the brain was then divided by the radioactivity injected and then multiplied by 100 to obtain the percentage value.

The cerebellum is a region with negligible density of D_2R [19,20]. The radioactivity in the cerebellum was therefore used as an approximate value for free and nonspecifically bound radioligand concentration in the brain.

The time curve for specific [^{11}C]MNPA binding to D_2R in high-density regions was defined as the difference between the total radioactivity concentration in a ROI and the cerebellum. Time for peak equilibrium was defined as the moment when the curve for specific binding reaches its maximum value [21].

The ratio of binding in a ROI to the cerebellum was calculated for the entire PET measurement. This ratio corresponds at the time of specific binding peak equilibrium to the binding potential and can be viewed as an index for the density of available receptors [22]. All calculations are based on the assumption that radioactivity in the brain represents an unchanged radioligand [23].

2.3. Plasma metabolite studies

The fractions of unchanged [^{11}C]MNPA and metabolites in monkey plasma during PET measurement were determined using an HPLC system method, previously developed for other PET ligands [24]. Venous blood samples of 2 ml were obtained at 4, 15, 30 and 45 min after injection of [^{11}C]MNPA. The blood samples were centrifuged at 2000×*g* for 2 min, and the plasma (0.5 ml) was mixed with acetonitrile (0.7 ml) and centrifuged again at 2000×*g* for 2 min. The radioactivity in the supernatant of the acetonitrile–plasma mixture (1.1 ml) was measured in a NaI well counter (extraction yield >95%), and 1 ml was injected to μ-Bondapak-C18 (300×7.8 mm, 10 μm) HPLC column. The HPLC system consists of a Hitachi D-7000 interface module, a Hitachi L-7100 pump, a Rheodyne injector (7125 with a 1.0-ml loop) and a Hitachi L-7400 absorbance detector (254 nm) in series with a Packard Radiomatic 150TR radiodetector equipped with a PET flow cell (600-μl cell). The mobile phases used were acetonitrile (A) and phosphoric acid (10 mM) (B) with a flow rate of 6 ml/min. The HPLC program was 0–5 min (A/B) 25/75 isocratic, 5– 6.5 (A/B) 25/75–10/90; 6.5–8 (A/B) 10/90 isocratic.

The radioactive peak of unchanged [^{11}C]MNPA was integrated, and the area under the curve (AUC) was expressed as a percentage of the sum of the AUCs of all radioactive peaks.

3. Results

3.1. Radiochemistry

The incorporation yield of [^{11}C]methyl iodide to [^{11}C]MNPA was approximately 75%, and total synthesis time was 30–35 min. [^{11}C]MNPA was purified by semi-preparative reversed-phase HPLC with a retention time of 6.5–8 min (Fig. 3). The retention time on the analytical reversed-phase HPLC system was 3–4 min, indicating a radiochemical purity better than 98%. The specific radioactivity obtained at the time of administration of [^{11}C]MNPA was approximately 350 Ci/mmol (13 GBq/μmol), and the radioactivity injected was 56–57 MBq corresponding to a total mass injection of 1.5 μg.

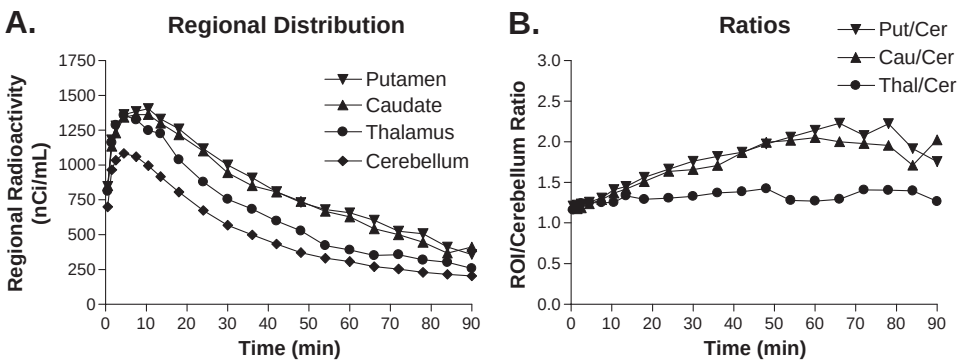

Fig. 5. (A) Time course for regional radioactivity (nCi ml^{-1}) in the brain of a cynomolgus monkey after iv injection of [^{11}C]MNPA. (B) Binding ratios.

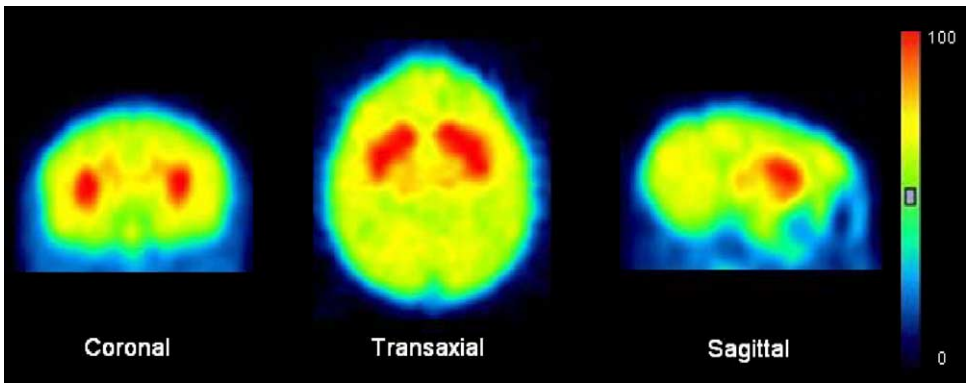

Fig. 6. Color-coded PET images showing the distribution of radioactivity in the monkey brain after injection of about 57 MBq [^{11}C]MNPA (measured between 9 and 93 min).

3.2. PET measurements

Following iv injection of [^{11}C]MNPA, total radioactivity in the brain peaked at 5 min at which time 4.5% of the injected radioactivity was in the brain. Highest uptake of radioactivity was seen in the striatum, uptake was moderate in the thalamus and low in the cerebellum (Figs. 5A and 6). The calculated binding ratio of the striatum or thalamus to the cerebellum increased during the first 70 min of the PET measurements (Fig. 5B). The maximum radioactivity ratio values of striatum and thalamus to the cerebellum were 2.23 ± 0.21 and 1.37 ± 0.06, respectively, which were reached at 78 and 72 min postinjection, respectively. The specific binding for all ROIs reached maximum between 10 and 30 min after injection of [^{11}C]MNPA (Fig. 7A).

The specificity of [^{11}C]MNPA binding to the D_2R was examined in a pretreatment study with raclopride. Following iv injection of unlabeled raclopride (1 mg/kg) 10 min prior to injection of [^{11}C]MNPA, the specific binding was markedly reduced (Fig. 7B). At 78 min, the striatum-to-cerebellum ratio was 1.26, as compared to 2.23 ± 0.21 in the baseline measurement, which corresponds to a 79% reduction after pretreatment.

3.3. Plasma metabolite studies

Blood samples were processed, and the plasma was isolated and extracted. After injection in the reversed-phase HPLC column, the fraction of unchanged [^{11}C]MNPA in plasma eluted within 6 min (recovery coefficient >98%). [^{11}C]MNPA was identified by coinjection of the authentic standard. The percentage of unchanged [^{11}C]MNPA in plasma 4 min after injection was about 50% and after 45 min about 20%. One radioactive peak eluting before [^{11}C]MNPA represented all radiolabeled metabolites together, and all metabolites were thus more polar than the parent compound.

4. Discussion

4.1. Radiochemistry

Direct alkylation with [^{11}C]methyl iodide of 2-OH-NPA is selective to the 2-OH position, which was confirmed by derivatization. Derivatization with acetic anhydride/pyridine and dibromomethane resulted in products that coeluted on HPLC with their reference compounds. Protection of the catechol group was therefore not needed. A plausible explanation for the selective labeling of the 2-OH position could be less sterical hindrance as compared to the 10- and 11-OH positions.

The synthesis gave a high incorporation yield of about 75%, and only minor amounts of unidentified radioactive peaks were seen (Fig. 3). Radiolysis was seen frequently, but only in small amounts (≤2%). Optimization of the

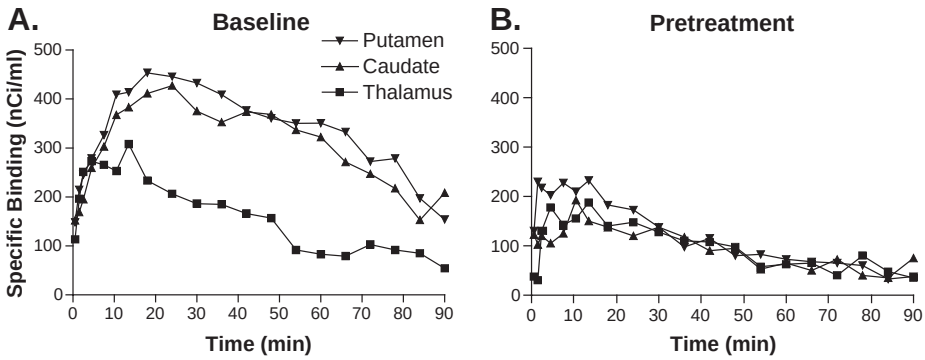

Fig. 7. Time course for specific binding (nCi/ml) in the brain of a cynomolgus monkey after iv injection of [^{11}C]MNPA in baseline (A) and pretreatment (B) conditions. In the pretreatment experiment, raclopride (1 mg kg^{-1}) was given iv 10 min before injection of [^{11}C]MNPA.

synthesis yield by replacement of [^{11}C]methyl iodide with [^{11}C]methyl triflate was not attempted because the incorporation yield was high.

4.2. PET measurements

Five minutes following injection of [^{11}C]MNPA, 4.5% ($n=2$) of the total injected radioactivity was present in the monkey brain. This uptake is higher than the 1–2% previously observed for [^{11}C]raclopride [25–27], a reference ligand that provides a good signal to quantify D_2R binding. Highest uptake was seen in the striatum, moderate uptake in the thalamus, while the level in the cerebellum was low. This regional distribution of radioactivity is in accordance with the known distribution of D_2R.

The specificity of [^{11}C]MNPA binding to D_2R was examined by a pretreatment measurement in which unlabeled raclopride was administered prior to injection of the radioligand. The radioactivity in regions known to contain D_2R was markedly reduced. This observation confirms that a large proportion of regional [^{11}C]MNPA binding represents specific binding to D_2R. Higher doses with the potential to displace all [^{11}C]MNPA binding were not used owing to animal safety precautions.

It should be noted that this pretreatment study with raclopride is not designed as a method to demonstrate selective binding of [^{11}C]MNPA to the high-affinity state of the D_2R. Raclopride is an antagonist and binds to the low- and high-affinity state of the receptor, where the agonist [^{11}C]MNPA theoretically only binds the high-affinity state. This study therefore does not provide conclusions about the affinity state of the receptor bound by [^{11}C]MNPA, but it demonstrates instead the selectivity of the [^{11}C]MNPA binding to the D_2R.

Thus far, data describing the in vivo pharmacological behavior of MNPA are not available, with the exception of in vitro radioreceptor assay reports [12,13]. However, MNPA is an analogue of the well-established DA agonist NPA, and we thus consider that MNPA behaves in vivo pharmacologically comparable to NPA.

The peak equilibrium time of [^{11}C]MNPA was 20–30 min in regions with a dense D_2R population (striatum), which is comparable to [^{11}C]NPA [8]. In comparison with [^{11}C]raclopride (42 min), the peak equilibrium time comes early, which optionally can result in shorter acquisition times in clinical studies.

One advantage with [^{11}C]MNPA, as compared to [^{11}C]NPA, is that the five times higher affinity may make it possible to also investigate the extrastriatally located low-density D_2R populations, such as in the thalamus. Following [^{11}C]MNPA injection at baseline conditions, there was a moderate uptake in the thalamus (thalamus-to-cerebellum ratio was 1.37 ± 0.06), which makes quantitative measurements in the thalamus feasible.

It cannot be ruled out that the relatively high injected mass (1.5 μg) may correspond to considerable receptor binding resulting in lower ROI-to-cerebellum ratios for the radioligand. Additional measurements with higher specific radioactivity (less mass) are thus required to fully evaluate the potential for D_2R binding in extrastriatal regions.

A second advantage of [^{11}C]MNPA in comparison with [^{11}C]NPA is that it is labeled by ^{11}C-methylation. This method is simpler than ^{11}C-propylation or ^{11}C-propionylation plus reduction, which is required for the labeling of [^{11}C]NPA. In addition, methylation systems are widely available and are automated in a full range.

MNPA has high affinity for the D_2-like receptor [12,13]. However, the affinity to the D_2R, D_3R and D_4R still remains to be examined. It is, however, not likely that the binding shown in the present study represents a significant degree of D_3R and D_4R binding since both these subtypes are expressed in low densities in the striatum and thalamus [19]. Furthermore, DA has an approximately 20 times higher affinity to the D_3R than to the D_2R [28,29], which may imply a high D_3R occupancy by endogenous DA and low receptor availability to radioligand binding [30].

[^{11}C]MNPA could be particularly advantageous in clinical populations with an aberrant function of the DA system. Thus far, only antagonists have been applied in clinical studies. Several of these studies have shown that an acute increase in synaptic DA concentration is associated with decreased in vivo binding of [^{11}C]raclopride and [^{123}I]IBZM. These studies used amphetamine, which stimulates dopamine release in vivo, and were performed in rodents, nonhuman primates, healthy human controls and in patients with different diseases [31–36]. Acute amphetamine administration given to schizophrenic patients induced a decrease in [^{11}C]raclopride and [^{123}I]IBZM binding, while such binding was elevated in untreated patients with schizophrenia, as compared to well-matched controls [31,33,35,36]. Patients with bipolar disorder and unipolar depression did not show changes in amphetamine-induced DA release [37,38].

We recognize the limitation associated with the use of DA antagonists in that they ultimately have no potential for distinguishing receptors in the high- vs. low-affinity state, especially as proportion varies with biological conditions. Subsequently, studying neurotransmission is difficult because endogenous DA binds preferentially to receptors in the high-affinity state. The development of D_2R imaging using radiolabeled agonists may thus prove to be crucial in order to better elucidate the specific aspects of DA neurotransmission in patients suffering from psychiatric and neurodegenerative disorders.

4.3. Plasma metabolite studies

No lipophilic, labeled metabolites of [^{11}C]MNPA were observed. The labeled metabolites obtained were polar and thus unlikely to pass the blood–brain barrier and contribute to the brain radioactivity.

5. Conclusion

[^{11}C]MNPA was successfully synthesized by a direct methylation approach. Preliminary PET studies showed uptake of radioactivity in brain regions known to contain D_2R. The specificity of [^{11}C]MNPA binding to D_2R was demonstrated by a pretreatment measurement which showed a marked reduction of binding after iv injection of unlabeled raclopride. [^{11}C]MNPA has potential as an agonist radioligand for the D_2-like receptor and has potential for examination of the high-affinity state of the D_2R in human subjects and patients with neuropsychiatric disorders.

Acknowledgments

The authors would like to thank the members of the Stockholm PET group for their assistance in the PET experiments. A grant from the Swedish Medical Research Council (41205-7) was used to support this work. Nick Seneca was supported by a grant from the NIH-KI joint PhD program. We are also grateful to Dr Cyrill Burger for providing the PMOD (version 2.5) software.

References

[1] Halldin C, Gulyas B, Langer O, Farde L. Brain radioligands — state of the art and new trends. Q J Nucl Med 2001;45(2):139–52.

[2] De Lean A, Kilpatrick BF, Caron MG. Dopamine receptor of the porcine anterior pituitary gland: evidence for two affinity states discriminated by both agonists and antagonists. Mol Pharmacol 1982;22:290–7.

[3] George SR, Watanabe M, Di Paolo T, Falardeau P, Labrie F, Seeman P. The functional state of the dopamine receptor in the anterior pituitary is in the high affinity form. Endocrinology 1985;117(2):690–7.

[4] Richfield EK, Penney JB, Young AB. Anatomical and affinity state comparisons between dopamine D_1 and D_2 receptors in the rat central nervous system. Neuroscience 1989;30(3):767–77.

[5] Seeman P, Grigoriadis D. Dopamine receptors in brain and periphery. Neurochem Int 1987;10(1):1–25.

[6] Sibley DR, De Lean A, Creese I. Anterior pituitary dopamine receptors. Demonstration of interconvertible high and low affinity states of the D-2 dopamine receptor. J Biol Chem 1982;257(11):6351–61.

[7] Cumming P, Gillings NM, Jensen SB, Bjarkam C, Gjedde A. Kinetics of the uptake and distribution of the dopamine D(2,3) agonist (*R*)-*N*-[1-(11)C]*n*-propylnorapomorphine in brain of healthy and MPTP-treated Göttingen miniature pigs. Nucl Med Biol 2003;30(5):547–53.

[8] Hwang DR, Kegeles LS, Laruelle M. (−)-*N*-[(11)C]propyl-norapomorphine: a positron-labeled dopamine agonist for PET imaging of D(2) receptors. Nucl Med Biol 2000;27(6):533–9.

[9] Mukherjee J, Narayanan TK, Christian BT, Shi B, Dunigan KA, Mantil J. In vitro and in vivo evaluation of the binding of the dopamine D_2 receptor agonist (11)C-(*RS*)-5-hydroxy-2-(di-*n*-propylamino)tetralin in rodents and nonhuman primate. Synapse 2000;37(1):64–70.

[10] Mukherjee J, Narayanan TK, Christian BT, Shi B, Yang ZY. Binding characteristics of high-affinity dopamine D_2/D_3 receptor agonists, 11C-PPHT and 11C-ZYY-339 in rodents and imaging in non-human primates by PET. Synapse 2004;54(2):83–91.

[11] Shi B, Narayanan TK, Christian BT, Chattopadhyay S, Mukherjee J. Synthesis and biological evaluation of the binding of dopamine D_2/D_3 receptor agonist, (*R*,*S*)-5-hydroxy-2-(*N*-propyl-*N*-(5′ -(18)F-fluoropentyl)aminotetralin ((18)F-5-OH-FPPAT) in rodents and nonhuman primates. Nucl Med Biol 2004;31(3):303–11.

[12] Gao YG, Baldessarini RJ, Kula NS, Neumeyer JL. Synthesis and dopamine receptor affinities of enantiomers of 2-substituted apomorphines and their *N*-*n*-propyl analogues. J Med Chem 1990;33(6):1800–5.

[13] Neumeyer JL, Gao YG, Kula NS, Baldessarini RJ. Synthesis and dopamine receptor affinity of (*R*)-(−)-2-fluoro-*N*-*n*-propylnorapomorphine: a highly potent and selective dopamine D_2 agonist. J Med Chem 1990;33(12):3122–4.

[14] Narendran R, Hwang DR, Slifstein M, Talbot PS, Erritzoe D, Huang Y, et al. In vivo vulnerability to competition by endogenous dopamine: comparison of the D_2 receptor agonist radiotracer (−)-*N*-[^{11}C]propyl-norapomorphine ([^{11}C]NPA) with the D_2 receptor antagonist radiotracer [^{11}C]-raclopride. Synapse 2004;52(3):188–208.

[15] Halldin C, Swahn CG, Neumeyer J, Hall H, Gao Y, Karlsson P, et al. Preparation of two potent and selective dopamine D-2 receptor agonists: (*R*)-[proply-^{11}C]-2-OH-NPA and (*R*)-[methyl-^{11}C]-2-OCH3-NPA. J Label Compd Radiopharm 1992;35:S265–6.

[16] Sandell J, Langer O, Larsen P, Dolle F, Vaufrey F, Demphel S, et al. Improved specific radioactivity of the PET radioligand [^{11}C]FLB 457 by use of the GE medical systems PETtrace MeI MicroLab. J Label Compd Radiopharm 2000;43:331–8.

[17] Wienhard K, Dahlboom M, Eriksson L, Michel C, Bruckbauer T, Pietrzyk U, et al. The ECAT EXACT HR: performance of a new high resolution positron scanner. J Comput Assist Tomogr 1994;18:110–8.

[18] Karlsson P, Farde L, Halldin C, Swahn C, Sedvall G, Foged C, et al. PET examination of [^{11}C]NNC 687 and [^{11}C]NNC 756 as new radioligands for the D_1-Dopamine receptor. Psychopharmacology 1993;113:149–56.

[19] Jaber M, Robinson SW, Missale C, Caron MG. Dopamine receptors and brain function. Neuropharmacology 1996;35(11):1503–19.

[20] Vallone D, Picetti R, Borrelli E. Structure and function of dopamine receptors. Neurosci Biobehav Rev 2000;24(1):125–32.

[21] Farde L, Eriksson L, Blomquist G, Halldin C. Kinetic analysis of central [^{11}C]raclopride binding to D_2-dopamine receptors studied by PET — a comparison to the equilibrium analysis. J Cereb Blood Flow Metab 1989;9(5):696–708.

[22] Mintun MA, Raichle ME, Kilbourn MR, Wooten GF, Welch MJ. A quantitative model for the in vivo assessment of drug binding sites with positron emission tomography. Ann Neurol 1984;15:217–27.

[23] Ito H, Hietala J, Blomqvist G, Halldin C, Farde L. Comparison of the transient equilibrium and continuous infusion method for quantitative PET analysis of [^{11}C]raclopride binding. J Cereb Blood Flow Metab 1998;18(9):941–50.

[24] Halldin C, Swahn C-G, Farde L, Sedvall G. Radioligand disposition and metabolism. In: Comar D, editor. PET for Drug Development and Evaluation. Dordrecht: Kluwer; 1995. p. 55–65.

[25] Farde L, Halldin C, Stone-Elmander S, Sedvall G. Analysis of human dopamine receptor subtypes using ^{11}C-SCH 23390 and ^{11}C-raclopride. Psychopharmacology 1987;92:278–84.

[26] Halldin C, Farde L, Högberg T, Hall H, Ström P, Ohlberger A, et al. A comparative PET-study of five carbon-11 or fluorine-18 labelled salicylamides. Preparation and in vitro dopamine D-2 binding. Nucl Med Biol 1991;18:871–81.

[27] Farde L, Pauli S, Hall H, Eriksson L, Halldin C, Högberg T, et al. Stereoselective binding of ^{11}C-raclopride in living human brain — a search for extra-striatal central D_2-dopamine receptors by PET. Psychopharmacology 1988;94:471–8.

[28] Sokoloff P, Giros B, Martres MP, Bouthenet ML, Schwartz JC. Molecular cloning and characterization of a novel dopamine receptor (D_3) as a target for neuroleptics. Nature 1990;347:146–51.

[29] Levesque D, Diaz J, Pilon C, Martres MP, Giros B, Souil E, et al. Identification, characterization, and localization of the dopamine D_3 receptor in rat brain using 7-[^{3}H]hydroxy-*N*,*N*-di-*n*-propyl-2-aminotetralin. Proc Natl Acad Sci U S A 1992;89(17):8155–9.

[30] Sovago J, Farde L, Halldin C, Langer O, Laszlovszky I, Kiss B, et al. Positron emission tomographic evaluation of the putative dopamine-D_3

receptor ligand, [^{11}C]RGH-1756 in the monkey brain. Neurochemistry 2004;45(5):609–17.

[31] Breier A, Su TP, Saunders R, Carson RE, Kolachana BS, de Bartolomeis A, et al. Schizophrenia is associated with elevated amphetamine-induced synaptic dopamine concentrations: evidence from a novel positron emission tomography method. Proc Natl Acad Sci U S A 1997;94(6):2569–74.

[32] Innis RB, Malison RT, al-Tikriti M, Hoffer PB, Sybirska EH, Seibyl JP, et al. Amphetamine-stimulated dopamine release competes in vivo for [^{123}I]IBZM binding to the D_2 receptor in nonhuman primates. Synapse 1992;10(3):177–84.

[33] Laruelle M, Abi-Dargham A, vanDyck CH, Gil R, D'Souza CD, Erdos J, et al. Single photon emission computerized tomography imaging of amphetamine-induced dopamine release in drug-free schizophrenic subjects. Proc Natl Acad Sci U S A 1996; 93(17):9235–40.

[34] Laruelle M, Iyer RN, al-Tikriti MS, Zea-Ponce Y, Malison R, Zoghbi SS, et al. Microdialysis and SPECT measurements of amphetamine-induced dopamine release in nonhuman primates. Synapse 1997; 25(1):1–14.

[35] Farde L, Wiesel FA, Stone-Elander S, Halldin C, Nordstrom AL, Hall H, et al. D_2 dopamine receptors in neuroleptic–naive schizophrenic patients. A positron emission tomography study with [^{11}C]raclopride. Arch Gen Psychiatry 1990;47(3):213–9.

[36] Abi-Dargham A, Gil R, Krystal J, Baldwin RM, Seibyl JP, Bowers M, et al. Increased striatal dopamine transmission in schizophrenia: confirmation in a second cohort. Am J Psychiatry 1998;155(6): 761–7.

[37] Anand A, Verhoeff P, Seneca N, Zoghbi SS, Seibyl JP, Charney DS, et al. Brain SPECT imaging of amphetamine-induced dopamine release in euthymic bipolar disorder patients. Am J Psychiatry 2000; 157(7):1108–14.

[38] Parsey RV, Oquendo MA, Zea-Ponce Y, Rodenhiser J, Kegeles LS, Pratap M, et al. Dopamine D(2) receptor availability and amphetamine-induced dopamine release in unipolar depression. Biol Psychiatry 2001;50(5):313–22.